nature medicine

Noninvasive optical imaging of apoptosis by caspase-targeted activity-based probes

Laura E Edgington[1,6], Alicia B Berger[1,6], Galia Blum[2,5,6], Victoria E Albrow[2], Margot G Paulick[2], Neil Lineberry[3] & Matthew Bogyo[1,2,4]

Imaging agents that enable direct visualization and quantification of apoptosis *in vivo* have great potential value for monitoring chemotherapeutic response as well as for early diagnosis and disease monitoring. We describe here the development of fluorescently labeled activity-based probes (ABPs) that covalently label active caspases *in vivo*. We used these probes to monitor apoptosis in the thymi of mice treated with dexamethasone as well as in tumor-bearing mice treated with the apoptosis-inducing monoclonal antibody Apomab (Genentech). Caspase ABPs provided direct readouts of the kinetics of apoptosis in live mice, whole organs and tissue extracts. The probes produced a maximum fluorescent signal that could be monitored noninvasively and that coincided with the peak in caspase activity, as measured by gel analysis. Overall, these studies demonstrate that caspase-specific ABPs have the potential to be used for noninvasive imaging of apoptosis in both preclinical and clinical settings.

As the number of therapies that function by inducing or inhibiting apoptosis continue to grow, imaging tools capable of tracking cell death will become increasingly crucial. Not unexpectedly, strategies for monitoring apoptosis have been developed on the basis of a wide range of surrogate biomarkers. These include specific apoptosis signaling molecules such as the caspases as well as markers of downstream events in the apoptosis cascade.

One commonly used probe of apoptosis, annexin V, is a protein with high affinity for phosphatidylserines exposed during the late stages of apoptosis. Annexin V has been labeled with a number of tags, including fluorochromes[1–3] and radioactive nuclides[4]. Labeled versions of annexin have been used for imaging studies in mouse models of human cancer[1] as well as for positron emission tomography and single photon emission computed tomography–based studies in humans[5–8]. Although annexin V represents a valuable label of apoptotic cells, its use in humans has had limited success partly as a result of its slow clearance *in vivo*, which leads to high background signals and incompatibility with radioactive nuclides with short half lives. As an alternative to annexin V, small amphipathic molecules that accumulate in apoptotic cells have been developed[9]. In addition, a radiolabeled analog of γ-carboxyglutamic acid ([^{18}F]-ML-10)[10] is currently entering clinical trials for positron emission tomography–based imaging studies of brain metastasis response to treatment (clinical trials NCT00791063, NCT00696943 and NCT00805636). However, the limited information regarding its mode of action makes it difficult to determine the overall applicability of this probe to diverse types of cell death observed in other disease systems.

As direct mediators of the early stages of apoptosis, caspases are obvious targets for molecular imaging probes. Because they are proteases, substrate processing can be used as a readout of activity. Currently, several classes of luminescent[11], fluorescently quenched[12] or radiolabeled[13] substrate-based probes are in development. Perhaps the biggest challenge for these probes is developing sequences that are specific for caspases. The substrate sequence most commonly used for these probes, Asp-Glu-Val-Asp, although optimal for caspase-3 and caspase-7 (ref. 14), is also efficiently recognized by several other cysteine proteases, including the cathepsins and legumain[15,16]. Cross-reactivity with cathepsins is especially problematic owing to their high constitutive expression in multiple tissues and organs including the liver, kidney and spleen. As a result, substrate-based reagents containing this or similar selectivity sequences may prove problematic for apoptosis imaging *in vivo*.

In addition to substrates, several classes of small-molecule inhibitors have been used to label caspase activity *in vivo*. These include reagents such as WC-II-89, a nonpeptidic competitive inhibitor derived from isatin sulfonamide analogs[17]; M808, an irreversible inhibitor based on a caspase substrate[17]; and fluorescently labeled peptide fluoromethyl ketones (FLICA probes)[18,19]. Although WC-II-89 has been shown to inhibit caspase activity *in vitro*, it remains difficult to determine its selectivity for caspases *in vivo*. Likewise, M808 has been shown to have substantial, nonspecific labeling in an *in vivo* model of cycloheximide-induced hepatocyte apoptosis[20]. The FLICA probes, in contrast, have been used mainly for FACS-based studies of apoptosis and are now commercially available. However, these probes suffer from lack of selectivity[21] and are effective inhibitors of various cathepsins[22]. We have also found that other fluoromethyl ketone–based probes of the caspases yield high levels of background labeling when used in simple *in vitro* apoptosis systems[15].

[1]Cancer Biology Program, [2]Department of Pathology, [3]Department of Immunology and [4]Department of Microbiology and Immunology, Stanford University School of Medicine, Stanford, California, USA. [5]Present address: School of Pharmacy, Faculty of Medicine, The Hebrew University, Jerusalem, Israel. [6]These authors contributed equally to this work. Correspondence should be addressed to M.B. (mbogyo@stanford.edu).
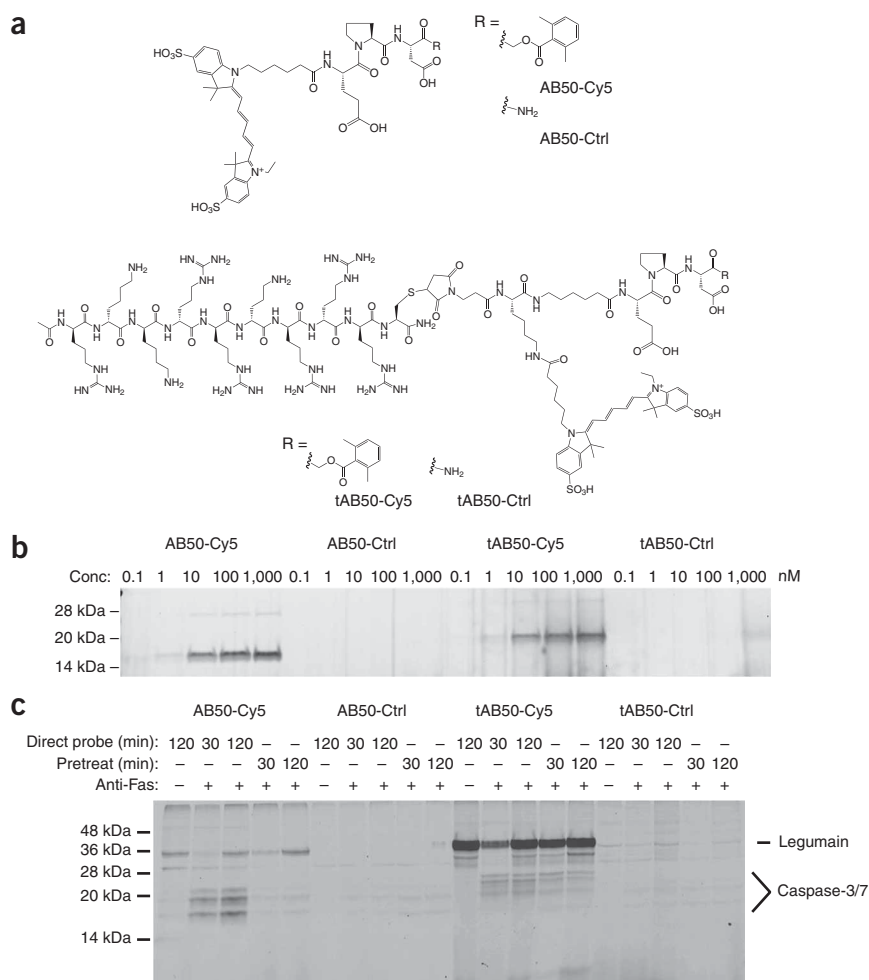
Figure 1 Biochemical evaluation of active and control probes. (**a**) Top, structures of the optimal caspase probe AB50-Cy5 and its control counterpart AB50-Ctrl that contains an amide in place of the AOMK reactive group. Bottom, structures of the Tat-labeled version of the AB50 probes. (**b**) Labeling of recombinant caspase-3 with the active and control probes from **a**. (**c**) Washout studies to monitor probe uptake. Intact Jurkat cells were either treated with the CH11 antibody to Fas (anti-Fas) and then labeled with each probe for the indicated times (direct probe) or pretreated with probes for the indicated times, followed by washout and addition of CH11 (pretreat). Cells were then lysed, and labeled proteins were analyzed by SDS-PAGE followed by scanning for Cy5 fluorescence with a flat-bed laser scanner.

We have previously described the development of irreversible inhibitors and active site probes of the caspases that show both broad and narrow selectivity within this family of proteases[23]. Although we initially found acyloxymethyl ketone (AOMK) probes designed based on our earlier work to be effective labels of caspases *in vivo*, these reagents showed marked cross-reactivity with cathepsins and legumain[23]. In this study, we identify optimal sequences that show lower legumain reactivity and a complete lack of reactivity toward the cathepsins. Notably, when these optimized probes were labeled with near-infrared fluorescent tags, they allowed caspase labeling to be monitored *in vivo* by noninvasive imaging methods. Furthermore, addition of a cell-permeable peptide sequence to the probe increased uptake into apoptotic cells, resulting in enhanced overall signal in apoptotic cells and tissues. Overall, these studies show that ABPs that target caspases can be used to track the early stages of apoptosis and that probe signal can be monitored using methods that allow whole-body, noninvasive imaging of apoptosis.

RESULTS

Evaluation and optimization of caspase ABPs

In our past studies, we designed a number of AOMK-based probes that showed efficient labeling of caspases in whole-cell extracts[23]. For our first generation ABP, we converted the most potent and broad-spectrum peptide sequence (AB28, containing the amino acid sequence 6-E-8-D) to a fluorescent probe by replacement of the P4 amino acid with a linker labeled with the with the near-infrared

fluorescent fluorophore Cy5. We initially tested this probe, AB46-Cy5, in a syngeneic lymphoma model in which tumorigenesis is driven by conditional overexpression of the *Myc* oncogene[24] (**Supplementary Fig. 1a,b** and **Supplementary Methods**). These initial studies indicated that the probe efficiently labels caspase-3 and caspase-7 but also labels cathepsin B and legumain (**Supplementary Fig. 1c,d**), consistent with previous studies[15,16]. To decrease cross-reactivity of AB46-Cy5 with cathepsin B, we made use of our earlier finding that the presence of a proline residue in the P2 position of legumain probes abolishes binding to cathepsin B[16]. Using this information, we developed an ABP containing a Glu-Pro-Asp acyloxymethyl ketone (EPD-AOMK) sequence labeled with the Cy5 fluorophore (AB50-Cy5); this probe showed labeling of caspase-3 and legumain with virtually no detectible cathepsin B labeling (**Supplementary Fig. 1e**). Indirect competition experiments produced similar results (**Supplementary Fig. 2**). To decrease the potency of our caspase probes toward legumain, we conducted a screen for P3 amino acids that direct selectivity away from legumain. We identified a series of sequences that enhanced potency toward caspase-3 and away from legumain (**Supplementary Fig. 3**). We synthesized a total of 11 inhibitors containing nonnatural amino acids that directed selectivity away from legumain (**Supplementary Fig. 4**). From this set of optimized inhibitors, AB53-Cy5, which contained a P3 biphenylalanine, showed the most selectivity toward caspases, with less than one-tenth as much legumain binding relative to AB46-Cy5 or AB50-Cy5 (**Supplementary Fig. 1**). However, labeling of intact cells indicated that it had relatively poor cell permeability (**Supplementary Fig. 5**). We, therefore, chose to carry out our *in vivo* studies with AB50-Cy5.

To enhance the cell permeability of AB50-Cy5, we synthesized a version of the probe containing a Tat peptide. This peptide makes use of multiple positively charged amino acids to carry attached cargo across membranes and has previously been used to increase the cell uptake of caspase substrates[12,13]. The Tat probe, tAB50-Cy5, differs from AB50-Cy5 in that the Cy5 fluorochrome is moved to a lysine side chain, and the Tat peptide is coupled through a cysteine residue to a maleimide group at the amino terminus of the probe (**Fig. 1a**). We also generated control versions of AB50-Cy5 (AB50-Ctrl) and tAB50-Cy5 (tAB50-Ctrl) that contain an amide in place of the reactive
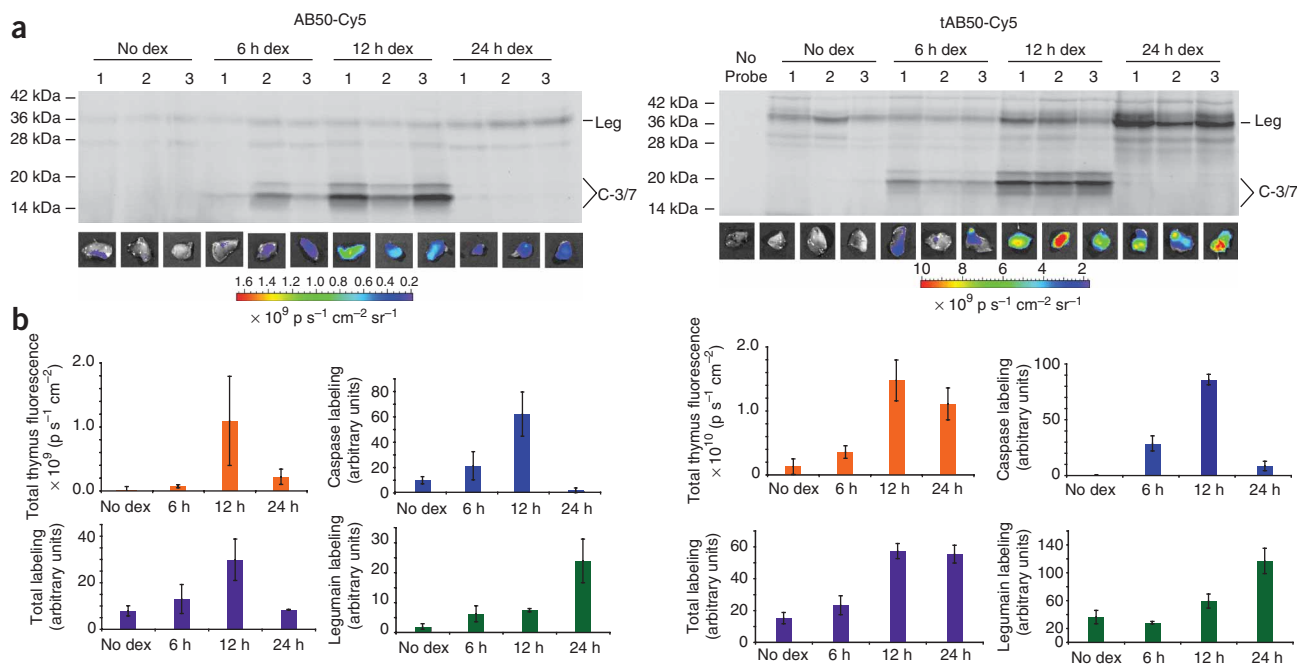
Figure 2 Kinetics of caspase activation in response to dexamethasone treatment. (**a**) *Ex vivo* images of thymus removed from mice treated with dexamethasone for indicated times and then injected with either AB50-Cy5 or tAB50-Cy5. The colorimetric scale shows photons per second per square centimeter per steradian (p s^{-1} cm^{-2} sr^{-1}) overlaid on bright-field images (bottom). After imaging, tissue extracts from intact thymi were analyzed via SDS-PAGE. Labeling of caspases and legumain is indicated. Leg, legumain; C-3/7, caspase-3 and caspase-7. (**b**) Quantification of intact thymus fluorescence relative to caspase and legumain labeling quantified from gel images. Fluorescence intensities from intact thymi are shown after background subtraction and normalization to thymus mass.

AOMK functional group. As expected, the active probes efficiently labeled recombinant caspase-3, whereas control versions of the probes did not (**Fig. 1b**). Note that the addition of the Tat peptide leads to a 2-kDa shift of the protease upon labeling. In addition, we tested all four probes for their ability to label caspases in intact cells treated with an antibody to Fas. We either activated cells by the Fas-specific antibody and directly labeled them with probes or pretreated them with probes and then washed them before activation of apoptosis (**Fig. 1c**). These results indicated that only the active probes AB50-Cy5 and tAB50-Cy5 label caspases, and, furthermore, only tAB50-Cy5 showed labeling of caspases after pretreatment and washout (**Fig. 1c**). However, we also found that addition of the Tat peptide resulted in a substantial increase in the labeling of legumain. This increase in labeling of a lysosome-resident protease is probably due to uptake of the probe via the endo-lysosomal route before release into the cytosol as has been suggested for similar carrier peptides[25].

### *In vivo* imaging of caspase activity in apoptotic thymocytes

To show the utility of caspase ABPs for imaging apoptosis, we monitored apoptosis in the CD4$^+$CD8$^+$ thymocytes of mice treated with dexamethasone[26]. We chose this system because the kinetics of apoptosis have been explored in previous studies using a number of common apoptosis markers including TUNEL[27] and annexin V[28,29]. We monitored caspase activation in mice treated with dexamethasone for 6, 12 or 24 h ($n = 3$ for each time point). We injected the AB50-Cy5 and tAB50-Cy5 probes intravenously 2 h before removal of thymi and imaging (**Fig. 2a**). After imaging, we processed the tissues and analyzed labeling in total extracts by SDS-PAGE followed by visualization of labeled proteins with a flat-bed laser scanner (**Fig. 2a**). This allowed us to biochemically characterize the target proteases labeled

by *in vivo* application of the probe. We confirmed by immunoprecipitation that the probes labeled both caspase-3 and legumain (data not shown). We then quantified total caspase and legumain labeling and compared these values to total fluorescence signals observed in intact thymi (**Fig. 2b**). These data indicate that legumain activity is low and remains largely unchanged in the first 12 h after dexamethasone treatment. Caspase-3 activity is observable at 6 h after treatment, peaking at 12 h and then sharply dropping to background levels at 24 h after injection (**Fig. 2b**). Notably, the overall trend in amounts of labeled caspases directly correlated with the overall signal observed for intact thymi using the IVIS system, suggesting that the fluorescence observed in whole organs can be used as a direct readout of total probe-labeled proteases. These data also agree with previous studies[27] that showed a peak in TUNEL$^+$ thymocyte staining 16 h after dexamethasone treatment followed by a sharp decrease at 18 and 24 h. These observations suggest that caspases are likely to be activated at early time points (that is, 6 h) and, therefore, may serve as effective markers of the early stages of apoptosis.

Comparison of the datasets for the AB50 and tAB50 probes suggested that although the overall trend in fluorescent signals in the intact thymi as well as the labeling patterns of caspases and legumain were the same for both, the overall signal intensity of labeled legumain and caspases as well as fluorescence emitted from intact thymi was increased for the Tat-labeled probe (**Fig. 2b**). Quantification of fluorescent signals indicated that peak fluorescence was greater in the tAB50-Cy5–labeled thymi (**Fig. 2b**). We did not observe a similar increase in tAB50-Cy5 signal in the samples treated with vehicle, suggesting increased uptake of the probe only into apoptotic cells (**Fig. 2b**). In further support of this hypothesis, we analyzed thymocytes from the 12-h time point by flow cytometry

Figure 3 Imaging dexamethasone-induced apoptosis in the thymus. (**a**) Quantification of total Cy5 fluorescence in thymi from mice treated with AB50-Cy5 or AB50-Ctrl for 50 min (left) or tAB50-Cy5 or tAB50-Ctrl for 5 h (right). Signals in both dexamethasone-treated and vehicle-treated samples are shown as total fluorescent signal normalized to tissue mass, as outlined in the Online Methods. (**b**) SDS-PAGE analysis of total thymus lysates from samples in **a**. Cy5 fluorescence was measured by scanning of the gel with a flatbed laser scanner. Labeling of caspases and legumain as well as signal from free probe is indicated. (**c**) Histology of thymus tissues from **a**. Tissues were stained with DAPI, and images were taken using a 10× or 40× objective (inset). Red indicates Cy5 fluorescence; blue indicates DAPI.
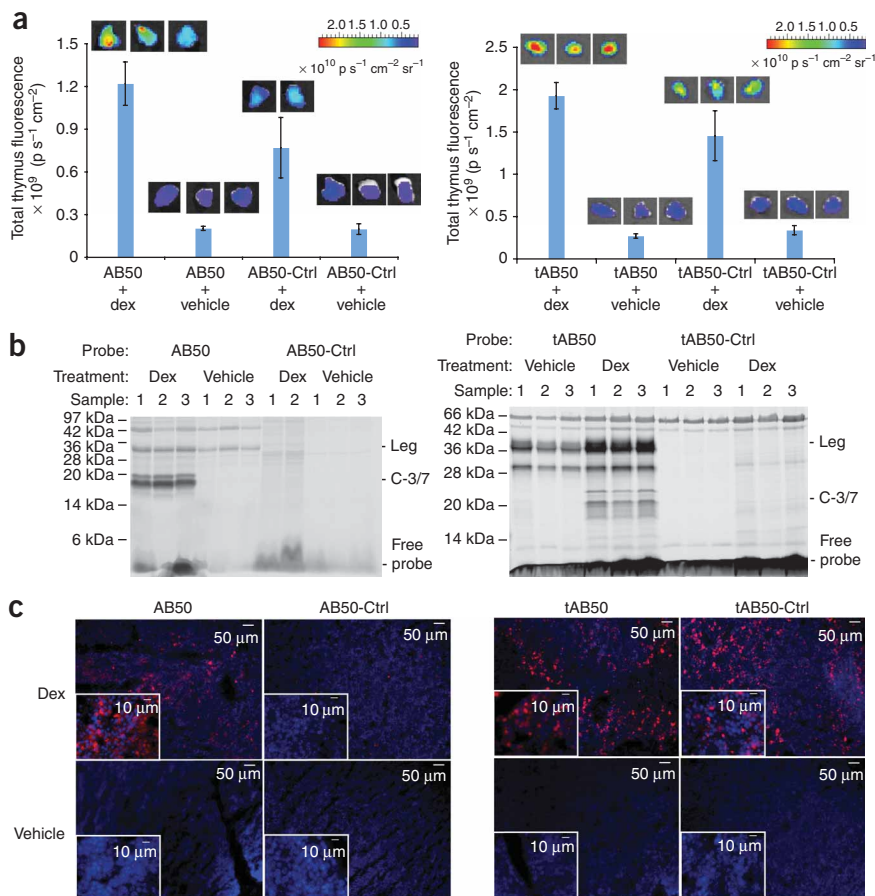
(**Supplementary Fig. 6**). This allowed us to monitor levels of Cy5 fluorescence in both apoptotic (that is, $CD4^+CD8^+$ thymocytes) as well as nonapoptotic cells (that is, $CD4^+$ or $CD8^+$ thymocytes). These data confirmed that dexamethasone treatment specifically induced apoptosis in $CD4^+CD8^+$ cells, as measured by a drop in this cell population over time. Furthermore, the tAB50-Cy5 probe accumulated only in dying cells, and probe-positive cells were also positive for annexin V (**Supplementary Fig. 6c**).

To further characterize the properties of our probes in the dexamethasone model, we monitored the uptake of active and control probes into intact thymi at 12 h after treatment with dexamethasone (**Fig. 3a**). These data indicated that both AB50-Cy5 and tAB50-Cy5 showed a highly significant accumulation in dexamethasone-treated thymi relative to vehicle-treated tissues ($P < 0.003$ for AB50-Cy5, $P < 0.0005$ for tAB50-Cy5). Of note, both control probes showed an accumulation in dexamethasone-treated samples, albeit at lower overall signal compared to the active probe (**Fig. 3a**). SDS-PAGE analysis of the total thymus extracts confirmed that the control probes failed to label either legumain or caspases, and these signals were therefore the result of an increase in levels of free probes in dexamethasone-treated samples (**Fig. 3b**). Thus, our ability to image apoptosis was enhanced by overall increased probe uptake into apoptotic cells. Finally, histology of thymus tissues showed that signals observed in tissue sections closely matched the signals observed for intact thymi (**Fig. 3c**). The signals for both the active and the control Tat probes showed strong nuclear staining of cells and only in dexamethasone-treated tissues (**Fig. 3c**). Therefore, we believe that there is considerable uptake of Tat-labeled probes when cells become apoptotic, and this uptake results in nuclear retention of the probes.

Noninvasive imaging of apoptosis in tumors treated with Apomab
In addition to the dexamethasone model, we wanted to evaluate our probes in a more relevant model of human disease. We therefore chose to monitor apoptosis in xenografted human tumor tissues that had been induced to undergo apoptosis by treatment with the monoclonal antibody Apomab. This reagent induces the extrinsic apoptosis pathway by binding death receptor-5 and is currently in phase 2 clinical trials as a chemotherapy agent for lung cancer[30,31]. We felt this was an

ideal model system, because the antibody induces apoptosis in a way that is highly distinct from the dexamethasone-induced intrinsic apoptosis in $CD4^+CD8^+$ thymocytes. As a starting point, we determined the *in vivo* kinetics of caspase activation in tumor cells in response to Apomab. We treated mice with Apomab, waited 2, 5, 8, 11 and 17 h and then injected AB50-Cy5 and allowed it to circulate for an additional hour. We then imaged whole tumors *ex vivo* and analyzed caspase labeling by SDS-PAGE (**Fig. 4a**). Quantification of total tumor fluorescence, as well as caspase and legumain labeling intensity, indicated that total fluorescent signals in the tumors closely mirrored levels of labeled caspase-3 and caspase-7, as measured by gel analysis (**Fig. 4b**). Furthermore, because the overall levels of legumain labeling were constant throughout the time course, this cross-reactivity did not hinder our ability to monitor dynamic changes in caspase activity. Overall, these results indicated that maximum caspase activity occurs 12 h after Apomab treatment.

Because each probe has a different clearance rate, we needed to determine the optimal time for imaging after probe injection. We therefore treated mice with Apomab or vehicle for 12 h, injected each of the active probes and noninvasively monitored tumor fluorescence over a range of time points (**Supplementary Fig. 7**). These data indicated that the Tat-labeled probes show substantially brighter signals but had slow clearance from all tissues, resulting in a low signal-to-background ratio at the early time points (**Supplementary Fig. 7**). We observed optimal contrast at 5 h after probe injection. AB50-Cy5, in contrast, cleared rapidly and showed a good signal-to-background ratio even at the early time points (that is, at 50 min). Thus, we monitored apoptosis in tumors 50 min after injection of
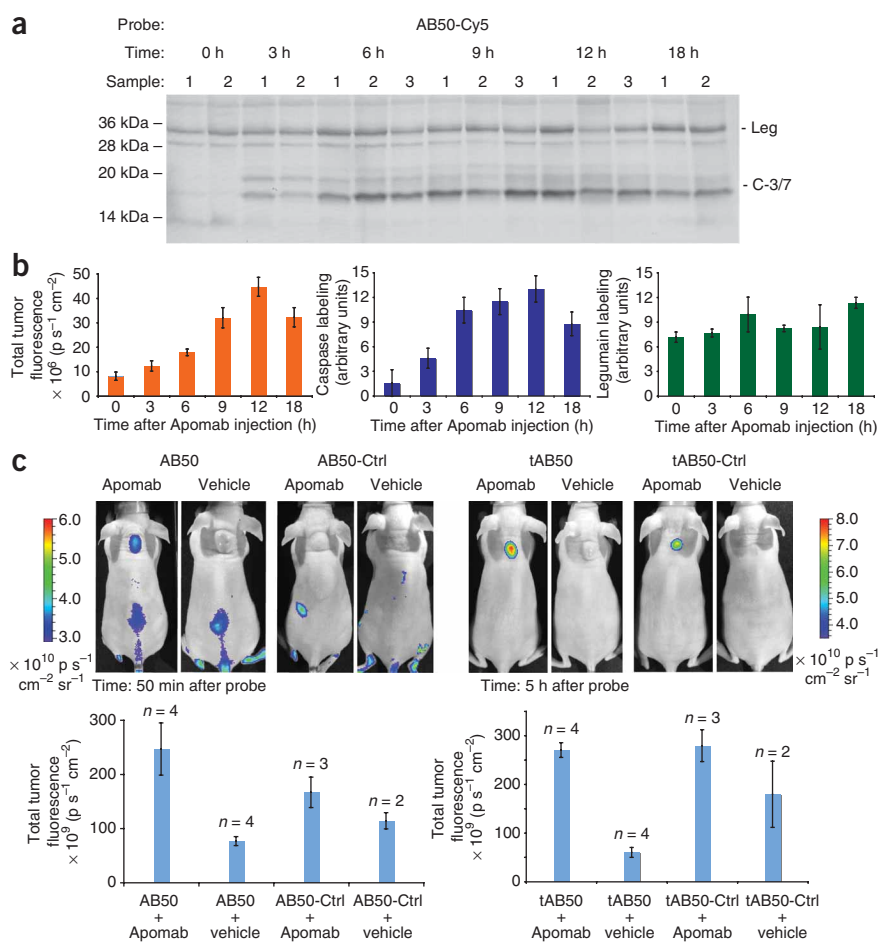
Figure 4 Noninvasive optical imaging of Apomab-induced cell death in mice bearing xenografted human colorectal cancer COLO205 tumors. (**a**) Analysis of the kinetics of Apomab-induced apoptosis in tumor tissues. Mice were treated with Apomab by intravenous injection, and AB50-Cy5 was injected at the indicated times. Tumors were removed, and lysates were analyzed by SDS-PAGE followed by scanning for Cy5 fluorescence with a flat-bed laser scanner. (**b**) Quantification of total fluorescence from whole tumors as a function of tumor surface area using the IVIS imaging system compared to the labeling intensities of caspases and legumain from gel images in **a**. (**c**) Noninvasive images of tumor-bearing mice treated for 12 h with Apomab or vehicle control and then with either control or active probes (top). Mean total fluorescence as a function of surface area is shown with s.e.m. Number of mice for each group is shown.

noninvasively monitor apoptosis in tumors treated with chemotherapy agents.

DISCUSSION

The development of reagents that can monitor apoptosis *in vivo* has potentially great value for monitoring therapeutic efficacy of drugs as well as for diagnosing early stages of diseases involving this key pathway. To address the need for new tools, several strategies have been implemented with mixed success. As the first responders to apoptotic stimuli, caspases are an ideal target for imaging agents for use in both preclinical and clinical applications. Here we described the development of fluorescent activity–based probes and their application *in vivo*. Starting from a first-generation probe, AB46-Cy5, that shows strong cross-reactivity with both cathepsins and legumain, we were able to improve selectivity of the probes toward caspases and show that they can be used to monitor apoptosis *in vivo* by both invasive and noninvasive methods. Additionally, because the probes covalently modify target proteases, they allow direct biochemical analysis of the kinetics of apoptosis *in vivo*.

In addition to finding that the caspase-specific probes can be used to monitor the kinetics of apoptosis in multiple model systems, we also found that control versions of the probes that lack the reactive AOMK functional group show some degree of specific uptake in apoptotic cells. We found that addition of the Tat peptide causes slower clearance and greater uptake into cells. However, we found markedly higher uptake of the Tat control probe compared to the non-Tat control. Histology of tissues from probe-treated mice showed that both active and control Tat probes accumulate in the nucleus, as has been proposed for the Tat peptide in other studies[32]. Although the control probes may still be capable of binding caspases as substrates, we believe that the use of Tat peptides may be beneficial for apoptosis imaging applications. Our results suggest that the non–Tat-labeled probes provide the best direct readout of caspase activity, but that the Tat-labeled probes boost overall specific signal and may therefore be useful for carrying other contrast agents into apoptotic cells.

Although we were able to develop a probe with lower legumain cross-reactivity, the overall degree of selectivity for caspases relative to legumain was modest. We believe that it may be difficult to completely

AB50-Cy5 and AB50-Ctrl and 5 h after injection of tAB50-Cy5 and tAB50-Ctrl (**Fig. 4c**). These images showed specific probe labeling of Apomab-treated tumors, with a high contrast for both tAB50-Cy5 and AB50-Cy5 (4.5-fold and 3.2-fold contrast, respectively; **Fig. 4c**). We also found that the control probes showed some degree of apoptosis-specific uptake into tumors. However, the AB50-Ctrl probe showed substantially weaker signal, and, overall, there was no significant difference in signals of Apomab-treated tumors relative to vehicle-treated tumors ($P \leq 0.27$). Notably, tAB50-Ctrl showed nearly identical accumulation in Apomab-treated tumors as tAB50-Cy5 but also produced higher background fluorescence in vehicle-treated tumors (**Fig. 4c**). Thus, although the control probes showed some accumulation in apoptotic cells, only the active probes showed a marked contrast between apoptotic and nonapoptotic tumors.

Finally, to confirm that the signal that we observed by noninvasive imaging was due to labeling of active caspases, we performed *ex vivo* imaging of intact tumors (**Fig. 5a**) followed by analysis of labeled proteins by SDS-PAGE (**Fig. 5b**). The *ex vivo* images closely matched the images obtained in live mice (**Fig. 5a**). In addition, gel analysis showed specific labeling of caspases only in Apomab-treated samples labeled with AB50-Cy5 and tAB50-Cy5 (**Fig. 5b**). We also confirmed specific labeling of apoptotic cells by histology of tumor tissues (**Fig. 5c**). In agreement with the results obtained for the dexamethasone model (**Fig. 3c**), we found that only tumor cells from Apomab treated animals showed probe staining (**Fig. 5**). Thus, these data demonstrate that caspase-specific probes can be used to
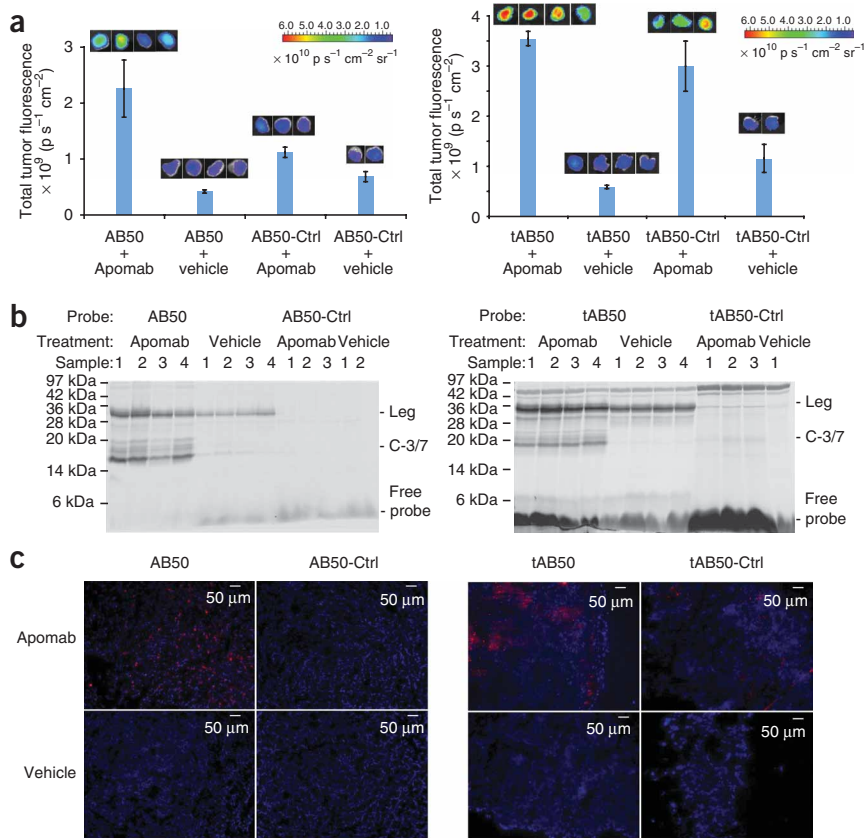
Figure 5 Biochemical and histological analysis of Apomab-induced apoptosis. (**a**) Images of excised tumors from mice treated with Apomab or vehicle and then treated with active and control probes. The mean total fluorescence normalized to tumor mass is shown with s.e.m. for each group of samples. (**b**) Fluorescence SDS-PAGE analysis of tumor tissues from **a**. Labeling of caspases and legumain as well as the signal from free probes is indicated. (**c**) Histology of tumor tissues. The other half of tumor tissues not used in **a** was frozen in OCT medium and sectioned. Tissues were stained with DAPI and images were taken with a 10× objective. Red indicates Cy5 fluorescence; blue indicates DAPI.

Overall, our data presented show that activity-based probes can be used for direct, non-invasive *in vivo* imaging of the kinetics of apoptosis in multiple mouse models. For both the dexamethasone and the Apomab systems, caspase activity can be detected at early time points, and it peaks at 12 h. This is in contrast to other markers of apoptosis such as annexin V and TUNEL staining, which serve as markers of the later stages of apoptosis. Thus, caspases are potentially useful markers for apoptosis *in vivo*, and agents that can be used to monitor dynamic changes in caspase activity are likely to have great value for both preclinical and clinical applications.

avoid cross-reactivity with legumain. However, labeling of this off-target protease can potentially be reduced by pretreatment with inhibitors that show exquisite specificity for legumain. For example, preblocking of legumain activity with aza-epoxide containing a P1 asparagine[33] should allow subsequent exclusive labeling of caspases by the AB50 probe series. Alternatively, it may not be necessary to use probes with absolute caspase selectivity for imaging apoptosis *in vivo*. We found that overall levels of legumain in the dexamethasone model seem to increase at late time points in the apoptosis cascade. This increase may be due to an increase in the overall number of legumain-expressing immune cells that respond to large numbers of dead or dying cells. Thus, probes that label both legumain and caspases may prove to be optimal for monitoring both early (caspase) and late (legumain) stages of apoptosis. Furthermore, the fact that legumain activity remains low and constant during the early stages of caspase activation suggest that probes can still be used to monitor dynamic changes in caspase activity at early time points. Finally, if tags such as Tat provide selective access to apoptotic cells, it may be desirable to have multiple targets that bind probes and lead to their long-term retention within the cell.

Although a number of methods have been explored to globally monitor levels of apoptosis, most make use of reporters that cannot be used to directly determine which protease targets are responsible for the production of a fluorescent or radioactive signal. One of the main benefits of the ABPs is their ability to form permanent covalent bonds with target proteases. Thus, signals can be imaged by noninvasive methods, and these signals can then be associated with specific target proteases by biochemical analysis of labeled tissues. In the two examples presented here, we show that overall labeling signals in whole tissues and in live mice correlate with the signal intensity of all labeled proteases in those tissues.

METHODS

Methods and any associated references are available in the online version of the paper at http://www.nature.com/naturemedicine/.

Note: Supplementary information is available on the Nature Medicine website.

1. Ntziachristos, V. *et al.* Visualization of antitumor treatment by means of fluorescence molecular tomography with an annexin V–Cy5.5 conjugate. *Proc. Natl. Acad. Sci. USA* **101**, 12294–12299 (2004).
2. Petrovsky, A., Schellenberger, E., Josephson, L., Weissleder, R. & Bogdanov, A. Jr. Near-infrared fluorescent imaging of tumor apoptosis. *Cancer Res.* **63**, 1936–1942 (2003).
3. Schellenberger, E.A. *et al.* Optical imaging of apoptosis as a biomarker of tumor response to chemotherapy. *Neoplasia* **5**, 187–192 (2003).
4. Blankenberg, F.G., Vanderheyden, J.L., Strauss, H.W. & Tait, J.F. Radiolabeling of HYNIC-annexin V with technetium-99m for *in vivo* imaging of apoptosis. *Nat. Protoc.* **1**, 108–110 (2006).
5. Belhocine, T. *et al.* Increased uptake of the apoptosis-imaging agent (99m)Tc recombinant human Annexin V in human tumors after one course of chemotherapy as a predictor of tumor response and patient prognosis. *Clin. Cancer Res.* **8**, 2766–2774 (2002).

6. Rottey, S., Slegers, G., Van Belle, S., Goethals, I. & Van de Wiele, C. Sequential 99mTc-hydrazinonicotinamide-annexin V imaging for predicting response to chemotherapy. *J. Nucl. Med.* **47**, 1813–1818 (2006).
7. Vermeersch, H. *et al.* 99mTc-HYNIC Annexin-V imaging of primary head and neck carcinoma. *Nucl. Med. Commun.* **25**, 259–263 (2004).
8. Hofstra, L. *et al.* Visualisation of cell death *in vivo* in patients with acute myocardial infarction. *Lancet* **356**, 209–212 (2000).
9. Aloya, R. *et al.* Molecular imaging of cell death *in vivo* by a novel small molecule probe. *Apoptosis* **11**, 2089–2101 (2006).
10. Cohen, A. *et al.* From the Gla domain to a novel small-molecule detector of apoptosis. *Cell Res.* **19**, 625–637 (2009).
11. Laxman, B. *et al.* Noninvasive real-time imaging of apoptosis. *Proc. Natl. Acad. Sci. USA* **99**, 16551–16555 (2002).
12. Bullok, K. & Piwnica-Worms, D. Synthesis and characterization of a small, membrane-permeant, caspase-activatable far-red fluorescent peptide for imaging apoptosis. *J. Med. Chem.* **48**, 5404–5407 (2005).
13. Bauer, C., Bauder-Wuest, U., Mier, W., Haberkorn, U. & Eisenhut, M. 131I-labeled peptides as caspase substrates for apoptosis imaging. *J. Nucl. Med.* **46**, 1066–1074 (2005).
14. Thornberry, N.A. *et al.* A combinatorial approach defines specificities of members of the caspase family and granzyme B. Functional relationships established for key mediators of apoptosis. *J. Biol. Chem.* **272**, 17907–17911 (1997).
15. Kato, D. *et al.* Activity-based probes that target diverse cysteine protease families. *Nat. Chem. Biol.* **1**, 33–38 (2005).
16. Sexton, K.B., Witte, M.D., Blum, G. & Bogyo, M. Design of cell-permeable, fluorescent activity–based probes for the lysosomal cysteine protease asparaginyl endopeptidase (AEP)/legumain. *Bioorg. Med. Chem. Lett.* **17**, 649–653 (2007).
17. Zhou, D. *et al.* Synthesis, radiolabeling and *in vivo* evaluation of an 18F-labeled isatin analog for imaging caspase-3 activation in apoptosis. *Bioorg. Med. Chem. Lett.* **16**, 5041–5046 (2006).
18. Bedner, E., Smolewski, P., Amstad, P. & Darzynkiewicz, Z. Activation of caspases measured *in situ* by binding of fluorochrome-labeled inhibitors of caspases (FLICA): correlation with DNA fragmentation. *Exp. Cell Res.* **259**, 308–313 (2000).
19. Smolewski, P. *et al.* Detection of caspases activation by fluorochrome-labeled inhibitors: multiparameter analysis by laser scanning cytometry. *Cytometry* **44**, 73–82 (2001).
20. Méthot, N. *et al.* A caspase active site probe reveals high fractional inhibition needed to block DNA fragmentation. *J. Biol. Chem.* **279**, 27905–27914 (2004).
21. Pozarowski, P. *et al.* Interactions of fluorochrome-labeled caspase inhibitors with apoptotic cells: a caution in data interpretation. *Cytometry A* **55**, 50–60 (2003).
22. Rozman-Pungerčar, J. *et al.* Inhibition of papain-like cysteine proteases and legumain by caspase-specific inhibitors: when reaction mechanism is more important than specificity. *Cell Death Differ.* **10**, 881–888 (2003).
23. Berger, A.B. *et al.* Identification of early intermediates of caspase activation using selective inhibitors and activity-based probes. *Mol. Cell* **23**, 509–521 (2006).
24. Felsher, D.W. & Bishop, J.M. Reversible tumorigenesis by MYC in hematopoietic lineages. *Mol. Cell* **4**, 199–207 (1999).
25. Richard, J.P. *et al.* Cellular uptake of unconjugated TAT peptide involves clathrin-dependent endocytosis and heparan sulfate receptors. *J. Biol. Chem.* **280**, 15300–15306 (2005).
26. Cohen, J.J. Glucocorticoid-induced apoptosis in the thymus. *Semin. Immunol.* **4**, 363–369 (1992).
27. Odaka, C. & Mizuochi, T. Macrophages are involved in DNA degradation of apoptotic cells in murine thymus after administration of hydrocortisone. *Cell Death Differ.* **9**, 104–112 (2002).
28. Brewer, J.A., Kanagawa, O., Sleckman, B.P. & Muglia, L.J. Thymocyte apoptosis induced by T cell activation is mediated by glucocorticoids *in vivo*. *J. Immunol.* **169**, 1837–1843 (2002).
29. Zavitsanou, K. *et al.* Detection of apoptotic cell death in the thymus of dexamethasone treated rats using [123I]annexin V and *in situ* oligonucleotide ligation. *J. Mol. Histol.* **38**, 313–319 (2007).
30. Adams, C. *et al.* Structural and functional analysis of the interaction between the agonistic monoclonal antibody Apomab and the proapoptotic receptor DR5. *Cell Death Differ.* **15**, 751–761 (2008).
31. Ashkenazi, A. Targeting the extrinsic apoptosis pathway in cancer. *Cytokine Growth Factor Rev.* **19**, 325–331 (2008).
32. Vivès, E., Brodin, P. & Lebleu, B. A truncated HIV-1 Tat protein basic domain rapidly translocates through the plasma membrane and accumulates in the cell nucleus. *J. Biol. Chem.* **272**, 16010–16017 (1997).
33. Sexton, K.B. *et al.* Specificity of aza-peptide electrophile activity-based probes of caspases. *Cell Death Differ.* **14**, 727–732 (2007).

ONLINE METHODS

Inhibitor and probe synthesis. We synthesized all inhibitors and ABPs by solid-phase synthesis methods previously reported for P1 Asp-AOMK compounds[23,34]. We coupled Cy5 fluorochrome (Invitrogen) to the molecules by a previously described method[35]. We coupled fluorenylmethyloxycarbonyl (Fmoc)–aminohexanoic acid (three equivalents) and maleimidopropionic acid (three equivalents) to the molecules using standard methods for coupling amino acids. The Tat peptide (Arg-Lys-Lys-Arg-Arg-Orn-Arg-Arg-Arg-Cys, all D-amino acids, except for the cysteine) was custom synthesized by the Stanford PAN peptide synthesis facility. We coupled Tat via its C-terminal cysteine to the amino-terminal maleimide in DMSO (100 mM final concentration) and DIEA (nine equivalents) while agitating in the dark. We monitored the coupling reaction every 30 min by liquid chromatography–mass spectometry analysis and purified it upon completion (typically after 2 h). AB50-Ctrl and tAB50-Ctrl were synthesized on Rink amide resin. We assessed the purity and identity of all compounds by LC-MS analysis using an Agilent HPLC coupled to an API 150 mass spectrometer (Applied Biosystems/SCIEX) equipped with an electrospray interface.

Ex vivo and gel-based analysis of dexamethasone-induced thymocyte apoptosis. All animal experiments were approved by the Stanford Administrative Panel on Laboratory Animal Care and strictly followed their specific guidelines. We obtained female 4–6-week-old BALB/c mice from the Stanford University Department of Comparative Medicine and housed them in the Research Animal Facility. We injected the mice into the peritoneal cavity with water-soluble dexamethasone (Sigma) dissolved (50 mg per kg body weight final dexamethasone concentration) in 100 μl sterile PBS 24, 12 and 6 h before killing. Two hours before killing, we injected the mice via tail vein with fluorescent probes (50 nmol) in 10% DMSO in sterile PBS (100 μl final volume). We anesthetized the mice with isoflurane and killed them by cervical dislocation. We collected thymi and visualized fluorescence using the IVIS 200 system with a Cy5.5 filter and Living Image software (Xenogen). We made thymus lysates using a bead beater in buffer containing 1% Triton X-100, 0.1% SDS, 0.5% sodium deoxycholate in PBS, pH 7.2, as described elsewhere[35]. We analyzed total protein lysate (100 μg) by SDS-PAGE using 15% polyacrylamide gels. We visualized probe labeling by scanning gels on a GE Typhoon flat-bed laser scanner (excitation 633 nm, emission 670 nm). For control probe experiments, we treated mice with dexamethasone for 11 h. We then injected the probes and allowed them to circulate for 50 min for non-Tat probes and 5 h for Tat probes. We then imaged one lobe of each thymus and analyzed by gel, and we used the other for histological analysis.

Noninvasive imaging and gel-based analysis of Apomab-induced apoptosis in xenografted tumors. We obtained female 6-week-old nude mice from Charles River and housed them in the Research Animal Facility. We injected

human colorectal cancer COLO205 cells (3×10^6) subcutaneously on the back of each mouse in 30 μl of 0.5% BSA in PBS. Tumors were established in 8–10 d. We administered Apomab (10 mg per kg body weight; Genentech) or vehicle (10 mM histidine, 0.8% sucrose and 0.02% Tween-20, pH 6) intravenously in a 100-μl volume as reported previously[30] for 2, 5, 8, 11 or 17 h. We then injected fluorescent probes (50 nmol) intravenously in 10% DMSO plus PBS in a 100-μl volume. After 1 h, we removed the tumors, imaged them with the IVIS 200 system and analyzed them by gel as described for the thymi. For noninvasive imaging, we injected mice with probe or control (50 nmol), anesthetized them with isoflurane and imaged them with the IVIS system over time. We determined the optimal time for probe clearance to be 50 min for non-Tat probes and 5 h for Tat-containing probes. We then removed the tumors, imaged them ex vivo and cut them in half. We processed one half for gel analysis and the other half for histology.

Histology. We fixed thymi on ice for 5 h in 4% paraformaldehyde and PBS, transferred them to a 30% sucrose solution and rocked them overnight at 4 °C, followed by embedding in OCT compound (Tissue-Tek). We placed the tumors directly into OCT compound without prior fixing. Frozen sections (10 μm) were cut by the Histology Lab in the Department of Comparative Medicine at Stanford. We revived the sections in PBS and mounted them with Vectashield Mounting Medium with DAPI (Vector Laboratories). We obtained images (10× and 40×) with a Zeiss Axiovert 200M microscope.

Labeling assays. We incubated recombinant caspase-3 (100 nM active in caspase buffer (100 mM Tris, 10 mM dithiothreonine, 0.1% CHAPS, 10% sucrose, pH 7.4)) with the fluorescent probes at a concentration range of 0.1–1,000 nM for 30 min. We analyzed samples as described above. For washout experiments, we pretreated Jurkat cells (5×10^6; American Type Culture Collection) with 1 μM AB50-Cy5, tAB50-Cy5 or their respective controls for 30 or 120 min followed by washing of the cells with warm RPMI three times. After washout, we added the CH11 antibody to Fas (Upstate Signaling Solutions) and incubated the cells for an additional 3 h. For non-pretreated samples, we treated Jurkat cells (5×10^6) with the antibody to Fas for 3 h with probe incubation for the last 30 or 120 min without washout. We lysed the cells on ice in hypotonic lysis buffer and analyzed labeled proteins as above.

Statistical analyses. Data are presented as averages, and error bars represent s.e.m. We determined statistical significance between treated and untreated samples using Student's *t*-test, and *P* values <0.05 were considered to be significant.

34. Lee, A. & Ellman, J.A. Parallel solution-phase synthesis of mechanism-based cysteine protease inhibitors. *Org. Lett.* **3**, 3707–3709 (2001).
35. Blum, G., von Degenfeld, G., Merchant, M.J., Blau, H.M. & Bogyo, M. Noninvasive optical imaging of cysteine protease activity using fluorescently quenched activity-based probes. *Nat. Chem. Biol.* **3**, 668–677 (2007).